

2-DIMENSIONAL UNSTEADY FLOW COMPUTATION OF FLOOD PROPAGATION IN CHANNELS

広島大学大学院 学生会員 OAlex George Mutasingwa
 広島大学工学部 フェロー会員 福岡捷二
 同上 正会員 渡邊明英

1. INTRODUCTION

It is important to understand flood propagation in rivers due to our desire to reduce and ultimately eliminate the loss of life and property in potentially inundated areas through accurate predictions. Accurate predictions are needed for channel designs, evaluation of span and height of bridges and flood relief management schemes to mention a few. Most rivers have cross sections that are compound with irregular and meander alignment, which complicate flood flow. Meandering and irregular channel causes unsteadiness of flood flow in rivers, which is characterized by time and space variation of flow parameters such as water discharge, velocity and water level. Analysis of such flood flows in a meandering channel is essential for evaluation of flood events as it depicts the real situation in nature. In this paper, first results of numerical model of unsteady flow in a single sine-generated meandering channel are compared with experimental results. The objective of the study is to understand different phenomenon occurring during flood flows. A 2-Dimensional depth averaged model has been constructed; it overcomes most spatial deficiencies encountered in 1-Dimensional models and has few parameters that are needed for calibration compared with 3-Dimensional models.

2. MODEL DESCRIPTION

Shallow water theory is accepted in most open channel flows, in which the effects of vertical accelerations are ignored. In this study, 2-Dimensional depth averaged unsteady flow equations have been derived from Navier Stokes equations (Chaudhry, 1993). Hydrostatic pressure distribution and small bottom slopes have been assumed. The governing equations obtained can be expressed as;

$$U_t + E_x + F_y + S = 0 \quad (1a) \quad \left(\frac{U}{J} \right)_t + \left(\frac{\psi_x E + \psi_y F}{J} \right)_\psi + \left(\frac{\eta_x E + \eta_y F}{J} \right)_\eta + \left(\frac{S}{J} \right) = 0 \quad (1b)$$

$$\text{where ; } U = \begin{bmatrix} Z \\ \bar{u}d \\ \bar{v}d \end{bmatrix} \quad E = \begin{bmatrix} \bar{u}d \\ \bar{u}^2d - \tau_{xx}d \\ \bar{u}\bar{v}d - \tau_{xy}d \end{bmatrix} \quad F = \begin{bmatrix} \bar{v}d \\ \bar{u}\bar{v}d - \tau_{xy}d \\ \bar{v}^2d - \tau_{yy}d \end{bmatrix} \quad S = \begin{bmatrix} 0 \\ -g_xd + gd \frac{\partial Z}{\partial x} + \tau_{bx} \\ -g_yd + gd \frac{\partial Z}{\partial y} + \tau_{by} \end{bmatrix}$$

$$J = 1/(\psi_x \eta_y - \psi_y \eta_x)$$

$Z = d + Z_b$ is the water level elevation, d is the flow depth, Z_b is the ground elevation, \bar{u} and \bar{v} are mean velocities over depth in x and y directions respectively, g = acceleration due to gravity, Turbulent shear terms are τ_{xx} , $\tau_{xy}(=\tau_{yx})$ and τ_{yy} . And boundary shear stress terms are τ_{bx} and τ_{by} .

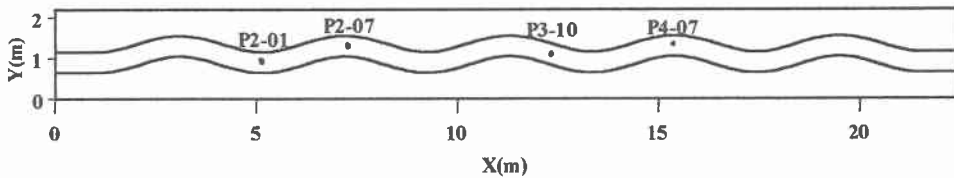


Figure 1: Channel Layout Plan

Coordinate transformation is done to incorporate the main channel boundaries accurately without the need of interpolations. The conservation form of the transformed equations in the natural coordinate system is indicated in 1(b). The depth averaged turbulent shear stress terms, τ_{xx} , $\tau_{xy}(=\tau_{yx})$ and τ_{yy} are determined as shown in equation (2). The effect of the wall is accounted using Molls et. al. (1998) approach, where the length at the wall is distributed in the hydraulic radius as seen in (3).

$$\tau_{xx} = 2\varepsilon \frac{\partial \bar{u}}{\partial x}; \tau_{xy} = \tau_{yx} = \varepsilon \left(\frac{\partial \bar{u}}{\partial y} + \frac{\partial \bar{v}}{\partial x} \right); \tau_{yy} = 2\varepsilon \frac{\partial \bar{v}}{\partial y}; \varepsilon = \frac{\kappa U_* d}{6}, \kappa = 0.41 \quad (2)$$

$$R = \frac{d}{\left(1 + \frac{(d_o + d_{NJ})}{NJ \times \Delta \eta_j}\right)} \quad (3)$$

Where: d_o and d_{NJ} are the water depth at the walls in the cross section, $\Delta \eta_j$ is the lateral spacing and NJ is the last computational node from node zero.

Bed Shear Stress terms τ_{bx} , τ_{by} and Manning's coefficient, n was determined as seen below.

$$\tau_{bx} = d \frac{g n^2 \bar{u} \sqrt{\bar{u}^2 + \bar{v}^2}}{R^{1/3}}; \tau_{by} = d \frac{g n^2 \bar{v} \sqrt{\bar{u}^2 + \bar{v}^2}}{R^{1/3}} \quad (4)$$

$$n = \frac{1}{\sqrt{g \left(6.0 + 5.75 \log_{10} \frac{R}{k_s}\right)}}$$

Numerical approach used to solve the 2-Dimensional depth averaged flow equations was MacComark scheme. The procedure is a two step explicit scheme that is accurate both in space and time. Upstream boundary conditions were measured discharge as a function of time while downstream condition was water depth as a function of time. A non-slip condition was used for the wall boundary. Artificial viscosity was added to damp any effect of truncation errors caused by replacing continuous governing equations with discrete equivalent.

3. MODEL APPLICATION

The model was verified using measured experimental data (Fukuoka et. al., 2000) for the single main channel only, seen in figure (1). The experimental channel was 22.5m long, 0.5m sine generated main channel width and length of one wave was 4.1m. Points located as P2-01, P2-07, P3-10 and P4-07 were used to verify the computations because they had measured experimental data. The results presented in figures 2-5, compares computed (cltd) with measured data (msd).

4. CONCLUSION

In this stage of model development, prediction capability of the model is investigated. The model was able to reproduce well the water depth experimental results for single channel flow as can be seen in figures 2, 4 and 5. Velocity computation also agreed well with measured data as can be seen in figures 3. Some variations in velocity were also observed these could be the result of depth averaging of velocity. Small discrepancies can be eliminated by fine tuning the model.

5. REFERENCES

- Chaudhry, M H, (1993), "Open Channel Flow", Pretence-Hall, Eaglewood-Cliffs, N.J, USA.
 福岡捷二, 渡辺明英, 岡部博一, 関浩太郎, (2000), 'Effects of Unsteadiness, Plan-form and Cross-sectional form of Channels on Hydraulic Characteristics of Flood flow, Ann. J of Hydraulic Engineering, JSCE, Vol. 44, pg867-872. (In Japanese)

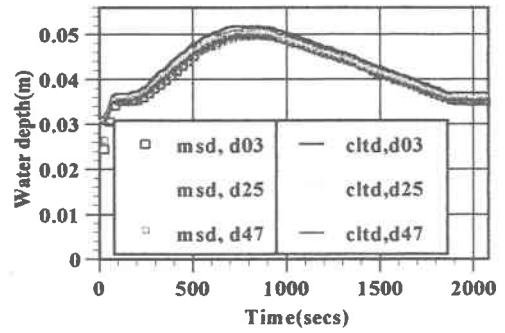


Figure 2: Water depth hydrograph at location P3-10

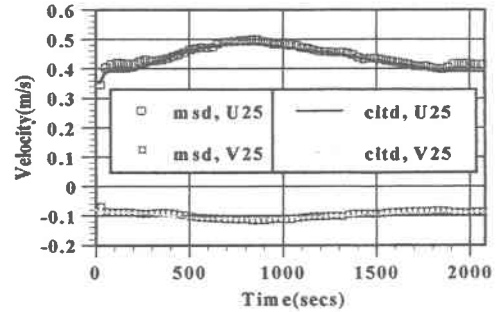


Figure 3: Velocity variation with time at location P3-10

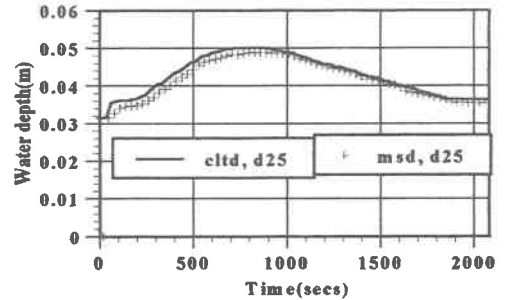


Figure 4: Water depth hydrograph at location P4-07

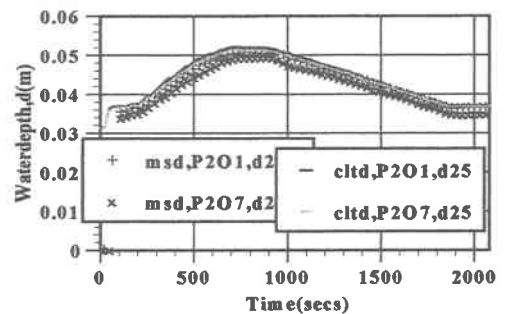


Figure 5: Water depth hydrograph at location P2-01 and P2-07

- Thomas Molls, Gang Zhao and Frank Molls, (1998), 'Friction Slope in Depth-Averaged Flow Model', ASCE, J of Hydraulic Engineering, Vol.124(6), pg81-85.